Continuum approach to discreteness

P. G. Kevrekidis
Theoretical Division and Center for Nonlinear Studies, MS B258, Los Alamos National Laboratory, Los Alamos, New Mexico 87545 and Department of Mathematics and Statistics, University of Massachusetts, Lederle Graduate Research Tower, Amherst, Massachusetts 01003-4515

I. G. Kevrekidis
Department of Chemical Engineering, Princeton University, 6 Olden Street, Princeton, New Jersey 08544

A. R. Bishop
Theoretical Division and Center for Nonlinear Studies, MS B258, Los Alamos National Laboratory, Los Alamos, New Mexico 87545

E. S. Titi
Department of Mathematics and Department of Mechanical and Aerospace Engineering, University of California, Irvine, California 92697-3875

(Received 4 November 2001; published 4 April 2002)

We study analytically and numerically continuum models derived on the basis of Padé approximations and their effectiveness in modeling spatially discrete systems. We not only analyze features of the temporal dynamics that can be captured through these continuum approaches (e.g., shape oscillations, radiation effects, and trapping) but also point out ones that cannot be captured (such as Peierls-Nabarro barriers and Bloch oscillations). We analyze the role of such methods in providing an effective ''homogenization'' of spatially discrete, as well as of heterogeneous continuum equations. Finally, we develop numerical methods for solving such equations and use them to establish the range of validity of these continuum approximations, as well as to compare them with other semicontinuum approximations.

DOI: 10.1103/PhysRevE.65.046613 PACS number(s): 05.45.−a

I. INTRODUCTION

In the past two decades, the role of discreteness in modifying the behavior of solutions of continuum nonlinear partial differential equations has been increasingly appreciated. Given that many of the physical contexts in which such models and their nonlinear dynamics are relevant, are inherently discrete in nature, understanding the role of discreteness becomes vital. Such physical contexts are quite diverse, ranging from the calcium burst waves in living cells [1] to the propagation of action potentials through the tissue of the cardiac cells [2] and from chains of chemical reactions [3] to applications in superconductivity and Josephson junctions [4], nonlinear optics and fiber arrays [5], complex electronic materials [6] or the local denaturation of the DNA double strand [7].

The realization of the important effects of discreteness (and, in particular, strong discreteness) emerged in the 1980s with the pioneering works [8–11] among others. This led to a large number of analytical and numerical studies (see, for instance, the review papers [12–16] and the references therein) of discreteness effects and of the notion of the so-called anticontinuum limit [17,18] (in which the lattice spacing $h \to \infty$) as well as of the coherent structure solutions and their properties close to that limit. In a number of recent developments [16], a host of analytical (such as the Evans function [19–22], singular perturbation theory [20,23,24], asymptotics beyond all orders [25], Hamiltonian dispersive normal forms [26,27], homogenization methods [28], and nonlinear stability analysis [29]), and numerical (such as bifurcation theory methods [30–32], iterative nonlinear eigenvalue methods [33] and numerical Evans and/or linear algebra methods [19]) techniques have been used to analyze the existence, stability, dynamics, and asymptotics of coherent structures in discrete problems.

In most of the above works the importance of treating the discrete problem directly has been recognized and emphasized, as discreteness has been found to trigger so-called ''radiation effects'' (see, e.g., [8,9,26,29]), which cause deceleration of the coherent structure in the lattice and eventually trapping and pinning [10,26,34] of the waves on a lattice site.

On the other hand, one may ask as to what extent continuum systems can capture such phenomenology. Another motivation for wishing to create continuum systems that mimic discrete effects is that continuum ordinary and partial differential equations are more easily amenable to analysis and, possibly, to the identification of potentially exact solutions. In fact, in the mathematical literature, there is a well-known technique for converting heterogeneous equations (i.e., continuum partial differential equations whose coefficients depend explicitly on space) to homogeneous ones with appropriately modified coefficients. This technique is called homogenization [35]. In a sense, discrete equations are a special kind of heterogeneous equations (this analogy has been analyzed in [36]) in which infinite weight (δ function weight) coefficients have been used on the sites of the lattice. Hence, developing such a continuum system mirroring the discrete properties would effectively constitute a form of homogenization analysis.

In view of the above motivations, Rosenau, in a series of

papers in the mid 1980s [37,38], developed a technique for providing continuum approaches to discreteness. In these works, he was able to give a systematic methodology for carrying out this program in one and also in higher spatial dimensions. He was also able to extract from the derived continuum equations useful information, such as dispersion relations, conservation laws, and even exact solutions in some special cases.

To the best of our knowledge such techniques, even though quite useful for analytical considerations (they are still used for extracting conclusions on discrete systems; see e.g., [39] for a recent example), have not been used very widely numerically, perhaps in part due to the presence of mixed (spatial and temporal) derivatives in the continuum equations that renders them relatively cumbersome to use for computational purposes.

In this paper, our goal is to revisit such methods from a different perspective (that of Padé approximants [40,41]) and to propose a natural way to generalize them, as well as to implement them in numerical computations. After presenting the method, we analyze a number of features of the discrete system dynamics that should be expected to be captured by this methodology, as well as some that (by construction) cannot. We also make the relevant connections to the work of Rosenau. We then turn to numerical computations and study how well the method can approximate the dynamics of the genuinely discrete system for the prototypical cases studied in many of the references given above, the so-called Frenkel-Kontorova model [42] (also known as the discrete sine-Gordon equation [8]); the simplest experimental realization of the latter is an array of coupled torsion pendula under the effect of gravity [43].

The paper is organized as follows. In Sec. II, we give the derivation of the model from a different perspective than the one given by Rosenau. In Sec. III, we make the connections with the previous work, give generalizations of the model, and present some of the advantages and disadvantages of such an approach. In parallel to the presentations of Sec. II and III, the numerical methods that will be used to solve the continuum problem are presented. In Sec. IV these methods are implemented in studying the discrete sine-Gordon equation and the results are compared with the original discrete problem. Finally, in Sec. V, we summarize and conclude.

II. CONTINUUM MODEL

The general setting of equations that will be studied here is given by the form

$$u_{n,\{t,tt\}}=\Delta_2 u_n+F(u_n), \tag{1}$$

where n indexes the lattice sites. In these equations $\{t,tt\}$ signifies that either one or two temporal derivatives can be present. The former case corresponds to one-component (discrete) reaction-diffusion equations, while the latter corresponds to discrete nonlinear Klein-Gordon equations. While we keep these classes of nonlinear equations in mind, it will be immediately obvious that similar considerations will be generalizable to any system bearing the discrete Laplacian $\Delta_2 u_n=(u_{n+1}+u_{n-1}-2u_n)/h^2$ (h is the lattice spacing). In fact, it will be shown how first derivatives can also be represented in the same approach. This, in fact, will be one of the advantages of the Padé approach. $F(u_n)$ is the substrate nonlinearity term, which stems from a potential $f(u_n)$ such that $f'(u)=-F(u)$.

Our starting point in this analysis will be the following identity (Taylor expansion) for analytic functions (see e.g., [44]):

$$u(x+m)=\exp(m\partial_x)u(x). \tag{2}$$

For such functions one can then express spatial discreteness as follows:

$$\begin{aligned} u_{n+1}+u_{n-1}-2u_n &\equiv[\exp(h\partial_x)+\exp(-h\partial_x)-2]u(x) \\ &\equiv 4\sinh\left(\frac{\partial_x}{2}\right)u(x,t). \end{aligned} \tag{3}$$

Now expanding $\exp(\pm h\partial_x)$ [41], we have

$$\begin{aligned} \exp(\pm h\partial_x)-1=&\frac{1}{2}h^2\left(1+\frac{h^2}{12}\partial_x^2+\cdots\right)\partial_x^2 \\ &\pm h\left(1+\frac{1}{6}h^2\partial_x^2+\cdots\right)\partial_x. \end{aligned} \tag{4}$$

Then, regrouping the terms in the manner of Padé [40,41] one obtains

$$\exp(\pm h\partial_x)-1\approx\frac{1}{2}\frac{h^2\partial_x^2}{1-\frac{h^2}{12}\partial_x^2}\pm\frac{h\partial_x}{\left(1-\frac{h^2}{12}\partial_x^2\right)^2}. \tag{5}$$

We now use the pseudodifferential operator approximation of Eq. (5) to convert the differential difference equation of Eq. (1) into a partial differential equation (PDE) as follows:

$$u_{\{t,tt\}}\approx\frac{\partial_x^2}{1-\frac{h^2}{12}\partial_x^2}u+F(u). \tag{6}$$

Notice, in passing, that here we have used the sum of the two expressions (with the different signs) of Eq. (5), in approximating the second difference (discrete Laplacian) through Eq. (3). However, note that the difference of the expressions with the different signs would give an approximation to the first difference. Hence, the Padé method presented herein can also be implemented in the case of PDE's with first-order spatial differences. We will revisit first-order differences is Sec. III, while calculating the potential energy of the system.

One can treat the PDE of Eq. (6) in two different ways. If we act on both sides of Eq. (6) with the operator $(1-a\partial_x^2)$, where $a=h^2/12$, we obtain

$$u_{\{t,tt\}}-au_{xx\{t,tt\}}=u_{xx}+(1-a\partial_x^2)F(u). \tag{7}$$

The general form of the resulting equation is, essentially, the same as the one obtained by Rosenau [37,38], with some differences that will be clarified in the following section. The most general form can be rewritten as

$$u_{\{t,tt\}} - a u_{xx\{t,tt\}} = u_{xx} + F(u) + G(u) \tag{8}$$

with $G(u) = -a[F''(u)u_x^2 + F'(u)u_{xx}]$. This is the resulting regularization equation stemming from the process to the leading-order approximation (to be revised in the following section).

In fact, following [37], when the nonlinear term $F(u)$ is bounded (this is the case, for instance, for the sine-Gordon model, but not necessarily for other nonlinear Klein-Gordon models; a counterexample would be the ϕ^4 model), the term $G(u)$ in Eq. (8) can be omitted without significant effect on the dynamics of the system. The term that is critical for the incorporation of the discreteness effects, as argued in [37,38], is the second (mixed-derivatives) term of the left-hand side of Eq. (8).

On the other hand, as mentioned in the Introduction, terms with higher derivatives, and even more so when these are mixed, can present a significant challenge in numerical investigations. We bypass such obstacles by considering the ''parent'' Eq. (6) rather than the ''daughter'' Eqs. (7) and (8). In particular, a crucial observation for the numerical methods developed and implemented herein is that the plane wave $\exp(ikx)$ is an eigenfunction *to all orders* of the operator ∂_x^2; hence it is also an eigenfunction of all of its rational forms. Therefore, using the Fourier decomposition of the field $u(x)$,

$$u(x) = \sum_k \exp(ikx)\hat{u}(k) \tag{9}$$

(the hat will be used to denote Fourier transform), with the appropriate wave numbers determined by the boundary conditions used in the numerical implementation, we can express the pseudodifferential operator of Eq. (6) as

$$\frac{\partial_x^2}{1 - \frac{h^2}{12}\partial_x^2} u(x,t) = \sum_k -\frac{k^2}{1 + ak^2}\hat{u}(k,t). \tag{10}$$

Hence, to solve Eq. (6), we use the following algorithm at each time step of the simulation: (1) Fourier transform the field; (2) form the term in the sum of Eq. (10) in Fourier space; (3) Fourier transform the latter field back into real space; and (4) time step the simulation by one integration step.

The last step can be performed with the integrator of one's preference. For the computations presented herein, results have been obtained with fourth-order explicit Runge-Kutta (RK) integrators and have also been validated with eighth-order RK methods (see Ref. [45]).

It should be noted that this approach towards solving equations of the form of Eq. (6) was certainly known to Rosenau [46], even though, to the best of our knowledge, it was not numerically implemented in the solution of nonlinear partial differential equations of that form.

III. ANALYTICAL CONSIDERATIONS AND EXTENSIONS

In this section, we provide the connection of the model to previous work, give straightforward generalizations of it and their numerical implementation, and discuss the advantages and shortcomings of such a continuum approach.

In particular, connecting the discussion of the preceding section to the work of Rosenau [37,38], we observe that he was mostly interested in models of the form

$$u_{n,tt} = \frac{T(u_{n+1}) + T(u_{n-1}) - 2T(u_n)}{h^2}, \tag{11}$$

where $T(u)$ in addition to its harmonic [i.e., linear in the setting of Eq. (11)] part could also have a nonlinear part [38]. The continuum limit for such equations is $u_{tt} = \partial_x^2 T(u)$. However, Rosenau also partially studied models with an on-site substrate nonlinearity [such as the Frenkel-Konotorova (FK) model] in Sec. III of [37].

In the former case [Eq. (11)], linearizing about a uniform steady state, and considering plane wave solutions of the form $\exp(i\omega t - ikx)$ to derive the dispersion relation, one obtains

$$\omega^2 = \frac{k^2}{1 + ak^2}. \tag{12}$$

Hence, the continuous spectrum will extend over the interval $\lambda \equiv \pm i\omega \in \pm i[0, \sqrt{1/a})$, of the imaginary axis of the spectral plane.

In the case of Eq. (6), where either first or second derivatives and a substrate nonlinearity are considered, when linearizing about a uniform steady state $u = u_0 (= \text{const})$, the following dispersion relation is obtained:

$$\{i\omega, -\omega^2\} = -\frac{k^2}{1 + ak^2} + F'(u_0). \tag{13}$$

We assume here (as is the case for the stable uniform steady states of the models of interest), that $F'(u_0) \leqslant 0$. Then the continuous spectrum will extend over the interval $\lambda \in (F'(u_0) - 1/a, F'(u_0)]$ for the dissipative (parabolic) first-order in time PDE, while it will consist of the intervals $\lambda \in \pm i[\sqrt{-F'(u_0)}, \sqrt{-F'(u_0) + 1/a})$ in the Hamiltonian case of the second-order (in time) PDE.

An important observation that holds true for both Eqs. (12) and (13) is that the continuous spectrum has an upper bound, as does the continuous spectrum for the proper discrete problem. This was underlined as a significant asset of the regularization method used in [37,38] with respect to other continuum approaches to discreteness. What was not emphasized, however, (and to which point we will return in our effort to improve on this model), was that the upper bound of the dispersion relation is $\sqrt{-F'(u_0) + 1/a}$, instead of $\sqrt{-F'(u_0) + 1/(3a)}$, an upper bound about twice as high (actually $\sqrt{3}$ times), in the case of $F'(u_0) = 0$. An additional argument in favor of the Eqs. (6)–(8) presented in [37,38], was that, contrary to what is the case for other continuum

approaches to discreteness (see below), the number of boundary conditions needed to solve these equations will be the same as the ones needed for the original discrete equation.

The most popular among the alternative methods that, in fact, need additional boundary conditions has been essentially the Taylor expansion of the discrete Laplacian. In particular, the general form of this Taylor expansion reads

$$\Delta_2 u_n = \sum_{j=1}^{\infty} \frac{2h^{2j-2}}{(2j)!} u^{(2j)} = u_{xx} + a u_{xxxx} + O(h^4). \quad (14)$$

In all of the cases in which the Taylor expansion has been implemented, only the leading-order fourth derivative term has been used. As pointed out by Rosenau, this term necessitates additional boundary conditions. However, it is not without reason that in all of the cases in which this equation has been discussed, it has been used either in a modified setting (through an appropriate transformation as was done in [47] and later in [48,49]), or it has been used to obtain static solutions and their stability [23,50]. The reason is straightforwardly found in the dispersion relation for the equation obtained by substituting the above expansion in Eq. (1),

$$-\omega^2 = -k^2 + ak^4 + F'(u_0). \quad (15)$$

Hence, for large wave numbers, the equation suffers an ''ultraviolet catastrophe,'' as excitation of these wave numbers will destabilize the system. We will also demonstrate this effect numerically in the following section.

The important question that arises next (also in view of the failure of the leading-order approximation to capture the upper bound of the continuous spectrum) is whether the continuum approximation can be improved. To accomplish that, one can consider, for instance, matching the Taylor expansion to higher order by a fraction of the form

$$\frac{\partial_x^2}{1 - \frac{h^2}{12}\partial_x^2 + \frac{h^4}{b}\partial_x^4} \approx \partial_x^2 \left[1 + \frac{h^2}{12}\partial_x^2 - \frac{h^4}{b}\partial_x^4 + \frac{h^4}{12^2}\partial_x^4 + O(h^6) \right]. \quad (16)$$

Selection of b in such a way that $-1/b + 1/12^2 = 2/6!$ will make the expansion accurate to $O(h^6)$, however, this is not an appropriate expansion for our purposes, as the large wave number (k) limit of the left-hand side of Eq. (16) is obviously incorrect. We should thus be interested in a form that has a well-defined large wave number limit. A natural generalization that has such a limit is given by the continued fraction method. For instance, consider

$$\cfrac{\partial_x^2}{1 - \cfrac{A\partial_x^2}{1 - \cfrac{B\partial_x^2}{1 - C\partial_x^2}}}. \quad (17)$$

This expression for large k has a well-defined limit [being equal to $-(1+B/C)/A$] and so will every expression that contains $2m+1$ fractions between $2m+2$ expressions that have a (second) derivative (and hence give, in $m+1$ pairs, a well-defined large k limit). Notice that this is a natural generalization of the Rosenau result (the case of $m=1$). Notice also, perhaps most importantly, that the computational cost of the algorithm given in the preceding section is *not* affected by the generalization presented here. In particular, the expression that has to be calculated instead of the one in Eq. (10) is rather [for the continued fraction of Eq. (17)]

$$\sum_k \cfrac{-k^2}{1 + \cfrac{Ak^2}{1 + \cfrac{Bk^2}{1 + Ck^2}}} \hat{u}(k,t), \quad (18)$$

which is an algebraic expression of the same computational cost as in the case of Eq. (10). Notice that in reaching the conclusion of Eq. (18), the eigenfuction nature (to all algebraic orders) of $\exp(ikx)$ for the operator ∂_x^2 has been crucial.

In order to use Eq. (17) in practice (i.e., for computational purposes), we convert the three fractions into one of the form

$$-\frac{k^2(1 - \alpha h^2 k^2)}{1 - \alpha h^2 k^2 - \beta h^2 k^2 + \gamma h^4 k^4}, \quad (19)$$

where a simple (algebraic) reduction of A,B,C to α,β,γ has been used. We then use Taylor expansion of the denominator to convert the expression of Eq. (19) into one resembling Eq. (14). By matching up to $O(h^6)$ to the exact Taylor expansion, we obtain three algebraic equations for α,β, and γ. In this way, we obtain a set of solutions for α,β, and γ. We use here the set $\alpha = -0.007\,912$, $\beta = -1/12$, and $\gamma = 0.002\,056$. It is clear that this process can be carried out to higher order without additional conceptual complications, even though the algebraic manipulations will become more cumbersome. However, the process is straightforward and can, in principle, be standardized. An additional benefit [to the matching of the Taylor expansion up to correction terms of $O(h^8)$] that should be highlighted here is the value $\alpha/(\gamma h^2) = 3.848/h^2$ of the upper bound for ω^2, which is much closer to the theoretical upper bound of $4/h^2$ than the prediction $12/h^2$ of the leading-order approximation presented in the preceding section. Of course all these estimates for ω^2 are in the case $F'(u_0) = 0$. The latter has to be subtracted from the upper bound if it is nonzero; however, it is clear that in either case, the higher-order approximation captures much better the value for the upper bound. It should be noted that somewhat similar considerations in the framework of regularization methods appeared in [51].

Continuing our analytical study of the properties of models such as the ones of Eqs. (6)–(8) and their generalizations, we study the so-called Peierls-Nabarro barrier. In the presence of genuine discreteness, it is well known [8,25,26,30] that the symmetry of translational invariance is broken. The nonequivalence of lattice configurations together with the in-

teger shift invariance of the lattice problem give rise to a periodic [9,34,52] potential energy barrier which, using a term coined from the theory of dislocations in solids [53], is called the Peierls-Nabarro (PN) barrier. In fact, the exponential increase of the height of this barrier [25,22] for strong discreteness is the principal reason for trapping and pinning of coherent structures in these "strongly" discrete settings. An important observation for the continuum-type models, such as the ones considered here, is that this barrier is not present. The most trivial way to observe this is to note that any of the continuum expressions used above contains derivatives, and hence is, by construction, translationally invariant. An alternative, less heuristic way to reach the same conclusion is by means of conservation laws as presented in [37]. Considering, e.g., Eq. (7) and integrating by parts over the spatial variable x, it can be found that $\int u_t dx = I_1$ is an integral of the motion, which in this case is the linear momentum. The conservation law is directly associated, via Noether's theorem [54], with a zero eigenfrequency (a Goldstone mode), which in turn means that the PN barrier is absent as the translational symmetry (associated with linear momentum) is preserved. The associated frequency would have to be nonzero in order for a PN barrier to exist. Finally, apart from these indirect proofs, there is a direct demonstration of the absence of the PN barrier, which we give here since we believe it is instructive.

The PN barrier appears if one uses the discrete or even the continuum solution in the discrete potential energy [55,56] parametrized by the position of the center x_0 of the solution. One then finds, to the leading-order approximation through the Poisson summation formula [9,55,56,36], a periodic barrier in x_0 with an exponentially small (in the lattice spacing h) prefactor. The exponentially small width of the barrier has been justified on various occasions [22,25,30,36] so we will not dwell on it here.

In our case of continuum models approximating the discrete case, if we use the continuum Padé approximation to the first-order difference as mentioned in Sec. II, we obtain

$$V[u] = \int dx \left[\left(\frac{\partial_x}{1 - a\partial_x^2} u \right)^2 + f(u) \right]; \tag{20}$$

we recall that $f' = -F$ and that the first term in Eq. (20) has been obtained by taking the difference between the plus and minus sign identities in Eq. (5). Notice that for simplicity of exposition, we have implicitly used the centered difference approximation to the first derivative for the discrete problem, but from our symmetry arguments given above, it is clear that the result we will obtain will be true independently of the selected discretization. We now observe that the term $\int dx f(u)$ can always sustain a change of variables $x \to x - x_0$ without creating a PN term (i.e., a term dependent on x_0). That leaves the first term for which we use the Fourier transform $u(x,t) = \int \exp(ikx)\hat{u}(k,t)$, to obtain

$$\int dx \left(\frac{\partial_x}{1 - a\partial_x^2} u \right)^2 = \int dx \left[\int dk \exp(ikx) \frac{ik}{(1 + ak^2)^2} \hat{u}(k) \right]^2. \tag{21}$$

One can now use the residue theorem for the integral over wave numbers. The poles are at $k = \pm k_0 = \pm i/\sqrt{a}$. The general formula states that

$$\int dk \frac{\hat{g}(k)}{(k - k_0)^m} = \frac{\hat{g}^{(m)}(k_0)}{(m-1)!}. \tag{22}$$

We thus obtain

$$\int dk \exp(ikx) \frac{ik}{a^2 (k^2 - k_0^2)^2} \hat{u}(k) = \frac{1}{a^2} \frac{d}{dk} \left(\frac{ik\hat{u}(k)\exp(ikx)}{(k - k_0)^2} \right) \Bigg|_{k=-k_0} + \frac{1}{a^2} \frac{d}{dk} \left(\frac{ik\hat{u}(k)\exp(ikx)}{(k + k_0)^2} \right) \Bigg|_{k=k_0}. \tag{23}$$

However, notice that if we perform the differentiation and the evaluation of the derivative terms at $k = \pm k_0$ and we then proceed to make a change of variables $x \to x - x_0$, the only type of terms containing x (and x_0) that will appear will be of the form $\exp[ik_0(x + x_0)]$, $\exp[-ik_0(x + x_0)]$, and the squares of such terms stemming from the square in Eq. (21). But all of these terms are rapidly oscillating and their integration over x will yield a vanishing result. Hence, there will be no PN barrier term as was clear also from the previous approaches. We believe that this demonstration is instructive in showing how first derivative terms and energy estimates can be evaluated in the general class of models considered herein.

A number of observations on the advantages and disadvantages of this class of continuum methods in approximating discreteness are in order.

A. Advantages

(i) These methods can capture the bounded nature of the continuous spectrum much better than previous ones (and, in fact, almost exactly upon the suitable generalizations considered herein). Also, the number of boundary conditions needed for well posedness is the same as that of the original discrete problem.

(ii) These methods embody the possibility for radiative losses. As is, in part, observed in the rather crude (since it involves traveling wave solutions, as the author points out) analysis of [39], for similar equations to the ones presented here, the kink profile will steepen in these continuum models. This adjustment of the kink shape is in agreement with

the observations of the original discrete problem. Furthermore, as we will emphasize in the Sec. IV, even though the translational modes do not bifurcate (translational invariance is preserved), edge (shape) mode bifurcations can and *do* occur. These internal modes bifurcating from the edge of the continuous spectrum generate a potential energy barrier, the oscillation in which (wobbling of the coherent structure) can provide radiation emission mechanisms similar to the ones presented in [26]. Hence, not only the shape adjustment but also the oscillation due to the edge mode can remove energy from the coherent structure and irreversibly transform it into small amplitude phonon excitations.

(iii) In view of comment (2), such equations as the ones considered above can exhibit pinning, if the kinetic energy is drastically reduced by radiative mechanisms, such as the one considered above.

(iv) Finally, PDE's of this form constitute a kind of ''homogenization'' of the discrete equations, preserving a significant amount of phenomenology present in the discrete system itself. An additional advantage is that this can also be useful in obtaining homogenized versions of heterogeneous continuum equations. This can be justified as follows: if we consider a heterogeneous equation of the form

$$u_{\{t,tt\}} = u_{xx} + F(u) + V_{ext}(x;h)u, \tag{24}$$

where $V(x;h)$ is an appropriate heterogeneous function [e.g., $V_{ext}(x;h) = \sin^2(2\pi x/h)$], then as has been indicated recently [57], a tight binding ansatz (or a Wannier function approach)

$$u(x,t) = \sum \psi_n(t)\,\phi(x - x_n) \tag{25}$$

can be used to convert (upon appropriate integrations over ϕ) Eq. (24) into a discrete equation for ψ_n of the form

$$\psi_{n,\{t,tt\}} = \Delta_2 \psi_n + \epsilon \psi_n + \Lambda F(\psi_n), \tag{26}$$

where $\epsilon \sim \int \phi^2(x - x_n) V_{ext}(x;h) + \phi(x - x_n)\,\phi_{xx}(x - x_n)\,dx$, and $\Lambda \sim \int f(\phi(x - x_n))dx$, in accordance with the derivation of [57]. Then, since for the discrete equation a continuum ''homogenization-type'' PDE can be derived as presented above, combining the heterogeneous to discrete and the discrete to (homogeneous) continuum steps, we can obtain such a ''homogenized'' PDE also starting from a heterogeneous continuum PDE.

B. Disadvantages

(i) There is no PN barrier in this model, as we showed above. This will significantly affect the phenomenology in the case of strong discreteness. The exponential increase of the PN barrier [8,25,26,22] is crucial in pinning coherent structures for strong discreteness. Even though the radiation phenomenology and the potential for internal mode resonances is present in the continuum model, we should expect to find trapping at considerably higher values of the lattice spacing than in the case of the original discrete model. In fact, this is what the numerical experiments will demonstrate in the following section.

(ii) An additional feature of the phenomenology of the discrete problem's dispersion relation that was not discussed in [37,38] is its periodic structure. The dispersion relation obtained in the continuum models presented herein as well as in [37,38] may have a saturation upper bound frequency but does not contain the periodic structure of multiple Brillouin zones that is present in the discrete system. Hence, as long as our interest is limited to the first Brillouin zone, the dispersion relation obtained matches very well that of the discrete problem. But, if a feature is to be studied that necessitates the presence of multiple Brillouin zones, this would be absent in the continuum approaches studied here. A feature of this type which is missed by the present approach, is, for instance, the phenomenon of Bloch oscillations of the discrete problem in the presence of an external linear potential. Such oscillations were observed theoretically for nonlinear models of the type presented here in [58,59]. In most of their experimental realizations (such as, semiconductor superlattices [60,61]), these oscillations appear in linear systems. However, they were recently observed in experiments with optical lattices for Bose-Einstein condensates [62] and were confirmed theoretically in the same context in [57]. Notice, in particular, in the collective coordinate analysis of [57] [Eq. (6) of [57]], the presence of a sinusoidal term that is responsible for the oscillations and which arises from the spatial periodicity of the discrete lattice. The absence of such periodicity, as is mirrored in equations of the type of Eq. (13), does not permit the presence of such phenomena in the context of continuum equations.

IV. NUMERICAL RESULTS

We now turn to numerical investigations of Eqs. (6)–(8) and the variants of Eqs. (16),(19), comparing the results with the direct results of the discrete problem of Eq. (1).

We solve the array of coupled ordinary differential equations of Eq. (1) directly by fourth order RK methods, while for the remaining equations, selecting the appropriate wave numbers for the implementation of free boundary conditions, we solve them through the algorithm given in Sec. II. The model for which the simulations are carried out is the discrete sine-Gordon equation. Hence the substrate nonlinear term is of the form $F(u) = -\sin(u)$. We will be interested in the dynamics of kinklike heteroclinic orbits in this model. In the continuum limit ($h \to 0$), the orbits have an explicit functional form

$$u(x,t) = 4\arctan\{\exp[\gamma(x - x_0 - vt)]\}, \tag{27}$$

where x_0 is the initial position of the kink and a Lorentz boost $x \to \gamma(x - vt)$, with $\gamma = \sqrt{1/(1 - v^2)}$ has been used to give the kink any initial subsonic speed v.

Figure 1 shows the results for $h = 0.5$. One concept that we use extensively to compare the discrete and continuum results is that of the projection of the continuum results onto the discrete lattice. This is done through the projection operator $P_n u(x,t) = \delta_{x,nh} u(x,t)$. The way in which this is implemented in practice is that the lattice of spacing h_1 which is used for the discretization of the continuum prob-

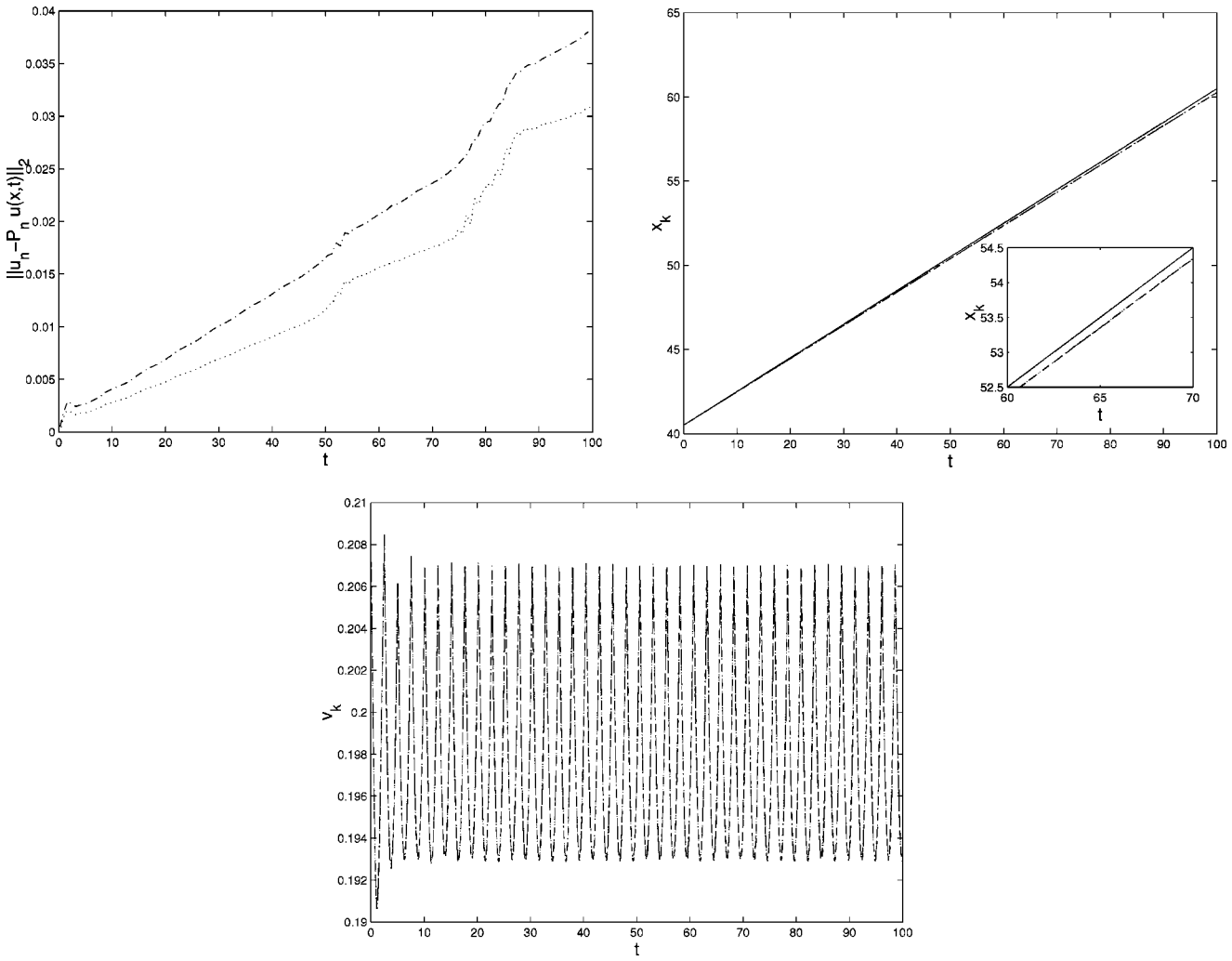

FIG. 1. The case of $h=0.5$. The top left subplot shows the time evolution of the norm $||u_n - P_n u(x,t)||_2$, where the projection of the continuum problem to the discrete one through the operator P_n is explained in the text. The dash-dotted line shows the result of the Rosenau approach, and the dotted one the generalized method of Sec. III. Notice a 20–25 % improved agreement in the latter case. The top right subplot shows the position of the kink for the initial condition, i.e., without a change in speed (solid line), the Rosenau approach (dash-dotted line), the generalized approach (dotted line), and the discrete problem (dashed line). Note the very good agreement between the discrete and continuum models (the latter three practically coincide). Finally the bottom center subplot shows the correspondingly evaluated kink speeds as functions of time. The line symbols remain the same in representing different approaches (dashed → discrete; dash-dotted → Rosenau approach; dotted → generalized approach). Notice once again that the results of the different approaches basically coincide. The same symbols have been used for the rest of the figures.

lem (hence, the condition $h_1 \ll h$ has to be satisfied), is chosen with an integer ratio of h/h_1; typically a ratio of $\approx 10-20$ is used in the simulations. Hence, $P_n u(x,t)$ shows the continuum profile every h/h_1 sites. This is a field of the same number of sites Nh as the discrete field and can be directly compared with the result of the discrete system. In particular a measure that we use in probing the accuracy of the continuum schemes is the L^2 norm $||u_n - P_n u(x,t)||_2$ of the difference between these two fields. In Fig. 1, for $h=0.5$, we can observe (in the top left panel) that the norm of the difference for the entire field never exceeds 0.04 in the Rosenau approach [as we will term Eqs. (6)–(8)] or ≈ 0.03 in the improved approach of Eq. (19) for the duration of the simulation. Thus, the behavior of the field is captured quite accurately in both approaches even though in the latter there is a gain in the accuracy of the order of 20–25 %. This will be a general observation in all of our numerical simulations: the generalized approach always yields results that are closer to the discrete behavior by $\approx 5-25$ % (depending on the value of h). In the top right panel, as another indicator of the accuracy of the results, the position of the kink is approximated by the interpolation method of [34]

$$x_k = h\left[n' + \frac{\pi - P_{n'}[u(x,t)]}{P_{n'+1}u(x,t) - P_{n'}u(x,t)} \right], \tag{28}$$

where n' is the site such that $P_{n'+1}u(x,t) > \pi$, while $P_{n'}u(x,t) < \pi$ (i.e., n' and $n'+1$ are the "sites" of the projection lattice nearest to the center of the kink). One can see

on the top right panel of Fig. 1, that the continuum methods of Eq. (6)–(8) and of Eq. (19) are in excellent agreement with the position of the exact discrete kink and only slightly deviate from the position that the speed would dictate (solid line) if it traveled with the initial velocity ($v_0=0.2$). Hence, the methods capture very accurately the ''adjustment'' of the kink's shape and speed to the discrete setting. Finally in the bottom left panel of Fig. 1, from the subsequent positions of the kink (and the time intervals between them), the speed of the kink is evaluated. The oscillation observed in all the different approaches *is* the Peierls-Nabarro oscillation, namely, the oscillation of the kink center as it travels between lattice sites. There is, however, a significant difference between the continuum approaches and the discrete result. In the original discrete case, the presence of the PN barrier is real, while in the case of the continuum model, it is an artifact of studying $P_n u(x,t)$ rather than the continuum field. In particular, as we will also mention below, an alternative method to calculate x_k but for the continuum field is to consider Eq. (28), with $h \to h_1$ and with $P_{n'} u(x,t) \to u(x=n' h_1, t)$ over the fine lattice of spacing h_1 (which represents the continuum in our case). If we were to probe this ''continuum'' x_k and its speed v_k, as we will see below, such (PN) oscillations would be absent.

Figure 2 shows the case of $h=0.9$. This is already considerable discreteness since it is well known that for $h \geqslant 1$, discreteness effects will become dominant, see, e.g., [8,26]. The top left panel once again shows the norm difference described above. It can be seen that even though it grows in time, up to $t=30$, it is ≈ 0.131 in the Rosenau approach and ≈ 0.111 in the generalized approach of Eq. (19). The reason for the increase in the norm can be traced in the top right and middle row left panel of Fig. 2, which shows the positions of the initial condition kink (solid line), the Rosenau approach (dash dotted), the generalized approach (dotted), and the discrete model (dashed), as well as the corresponding speeds. What is happening is that gradually the discrete kink is lagging behind the kinks of the continuum approaches, opening a gap between the spatial profiles of the two kinks, as we will see below. This gap is responsible for the norm increase of the difference of the fields. Viewing the left panel of the bottom row, it becomes evident why the discrete kink lags behind. One can verify that the barrier observed is the PN barrier. A rough estimate of subsequent maxima at $t_1 = 11.875$ and $t_2 = 16.575$ and an estimate of the period $T = t_2 - t_1$ multiplied by the approximate speed of $v_k \approx 0.192$ gives a spatial scale of $h=0.9024$, which clearly matches the lattice spacing. However, as has been argued previously, this barrier is present for the discrete system, while it is an artifact of the projection operator in the continuum case, where it is absent. However, the presence of this barrier, as has been analyzed in [8,26] entails a resonance mechanism. The so-called translational frequency $\omega_t = 2\pi v_k / h$ associated with the barrier, and its harmonics resonate with the extended wave phonon modes, as has been detailed in [8,26]. These resonances drain away the kink's kinetic energy converting it to phonons. Since in the case of continuum models this mechanism is absent, the decay of kinetic energy (seen in the dashed line of the bottom row left subplot) is not observed in the dash-dotted and dotted lines corresponding to the continuum models. Also in the same plot of kink speed as a function of the time, the ''continuum'' kink's speed defined above is given by the thick dots. This continuum speed v_c is analyzed in the right subplot of the top row of Fig. 2. It is calculated in both cases for the continuum model of Eq. (19), but with two different fine lattice spacings ($h_1 = h/10$ corresponds to the dashed line, while $h_1 = h/20$ corresponds to the solid line). In the former case, the average speed is very slightly lower $\langle v_c \rangle \approx 0.1923$, while in the latter it is $\langle v_c \rangle \approx 0.1926$. It can be clearly discerned in the figure as well as in the inset that two oscillations are superposed. Since this is for the continuum model, neither of the two is the discrete model PN oscillation of frequency ω_t. The fast oscillation has a period of $T \approx 0.467$, very close to h_1 / v_k when $h_1 = h/10$, while it is approximately half of that (≈ 0.234) when $h_1 = h/20$. Hence, this is the fast oscillation due to the very weak PN barrier of the *fine* lattice.

The slow oscillations, as is clear from the inset, are of the same frequency in both cases. This frequency can be found to be $\omega_e \approx 0.95$. This is a frequency for which $\omega_e < \omega_b = 1$, where ω_b is the frequency of the bottom edge of the continuous spectrum. Hence, it pertains to the shape oscillation of the kink due to the edge mode that has bifurcated from the band edge of the continuous spectrum [23,20–22]. Finally, in the middle and bottom row right subplots of Fig. 2, as a final diagnostic, the field's spatial profile is shown at an early time ($t=24$) and at a later time ($t=48$). The dashed line once again represents the discrete result, the dash-dotted line the Rosenau approach, and the dotted line the generalized continuum approach. In the first case (middle row), the continuum and discrete kinks are found to almost coincide. In fact the coincidence of the front fields (the field's detail as it approaches the front steady state $u_0 = 2\pi$) is rather remarkable, while the back field (approach to the steady state $u_0 = 0$) is captured less accurately and ''radiation'' of the discrete field is more intense than in the continuum case. This last observation can be understood as follows. The kink initially emits radiation both in the front and in the back, trying to adjust its shape and speed in the discrete setting. This feature is present both in the discrete and continuum situations. However, as time evolves and the kink moves, in the discrete situation it encounters the constraint of having to traverse the PN barriers, and in doing so sheds radiation through losing a fraction of its kinetic energy (the mechanism mentioned above), while in the latter continuum case, this mechanism is absent and only smaller amounts of radiation are generated through the resonance of the edge mode oscillations. Hence, gradually the discrete kink lags behind the continuum ones (bottom right subplot), which explains the increase of the norm of the difference between the two fields observed in the top left subplot of Fig. 2. The same argument accounts for the continuing accuracy of capturing the front field, as opposed to the increasing inaccuracy in the capturing of the back field: as more PN barriers are traversed more back field phonon radiation is generated.

For comparison in this case ($h=0.9$), we also performed simulations with the continuum approach of Eq. (14), which bears the potential for the ''ultraviolet catastrophe'' men-

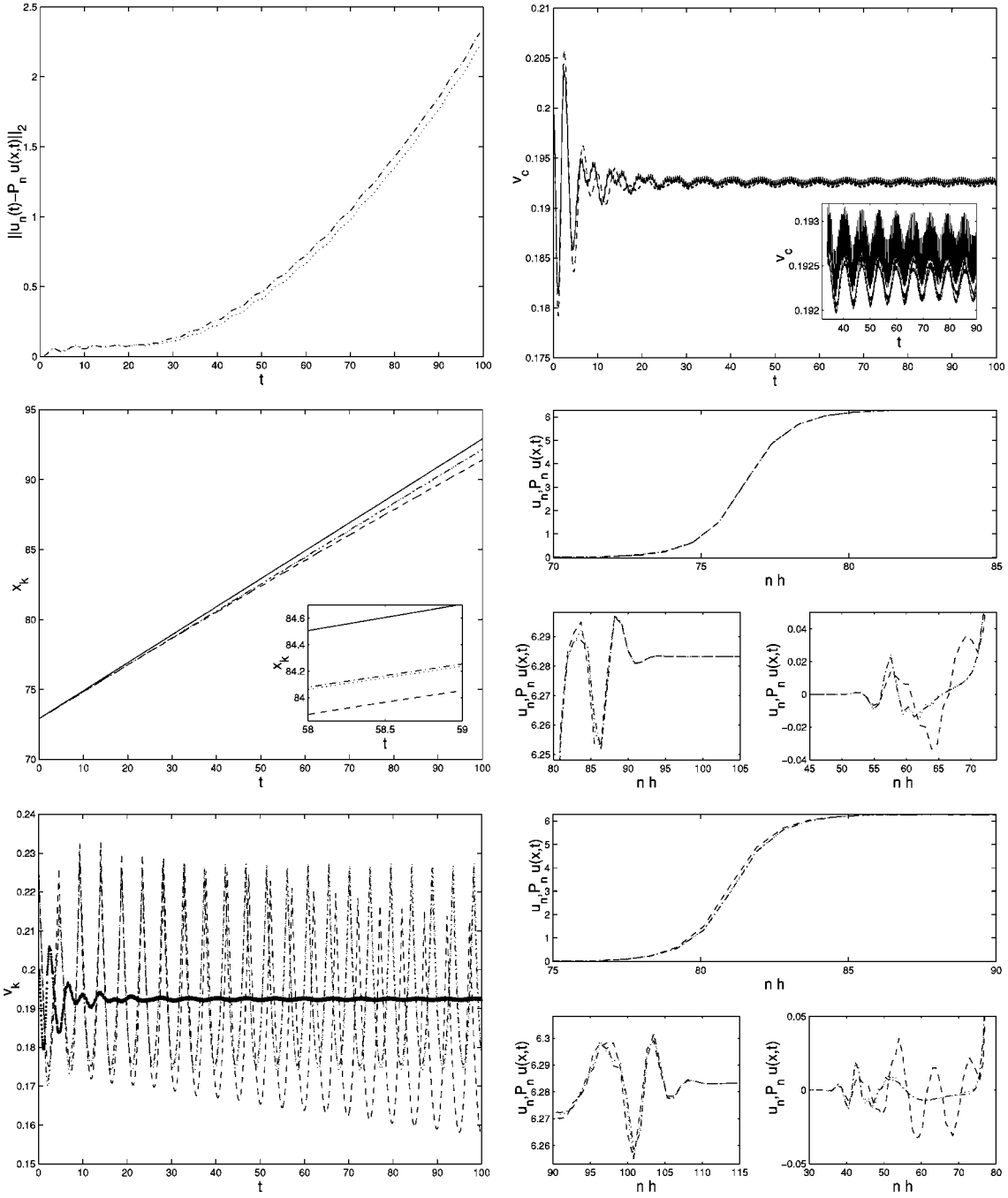

FIG. 2. The right subplots are the same as in Fig. 1, but for $h=0.9$. In the bottom left subplot a thick dotted line has been added to show the continuum speed of the generalized approach (rather than the one projected on the discrete lattice through P_n). See also the explanation in the text. In this case, we observe that even though the generalized approach is still better than the Rosenau approach, both move faster than the discrete kink. The reason is, as explained in the text, the presence of the PN barrier in the discrete case, which induces kinetic energy depleting resonances that in turn decrease the kink speed. This is clearly observed in the bottom row left subplot. On the contrary, the continuum models, as is shown, for instance, in the top right subplot showing the time evolution of the ''continuum'' speed (defined in the text), have no real PN barrier and hence their kinetic energy is not affected by that mechanism; hence, the continuum speed is almost constant. The continuum speed is shown in the middle right subplot for the generalized model in the cases of $h_1=h/10$ (dashed line) and $h_1=h/20$ (solid line). The clearly discernible superposition of two oscillations in the figure comes from the PN barrier of the fine scale (h_1; the fast oscillation) and the shape mode oscillation of $\omega_e \approx 0.95 < \omega_b$ (the slow oscillation). Finally the middle and bottom right panels show two snapshots of profiles of the field (the discrete field and the discrete projection of the continuum field). The line symbols are the same as in Fig. 1. The middle right panel is for $t=24$ while the bottom right is for $t=48$. Notice that in either case, the radiation field in front of the kink is very accurately captured, while in the back of the kink it is increasingly less accurately captured. For the explanation of this phenomenon, as well as of the gradual lagging behind of the discrete kink, see Sec. IV.

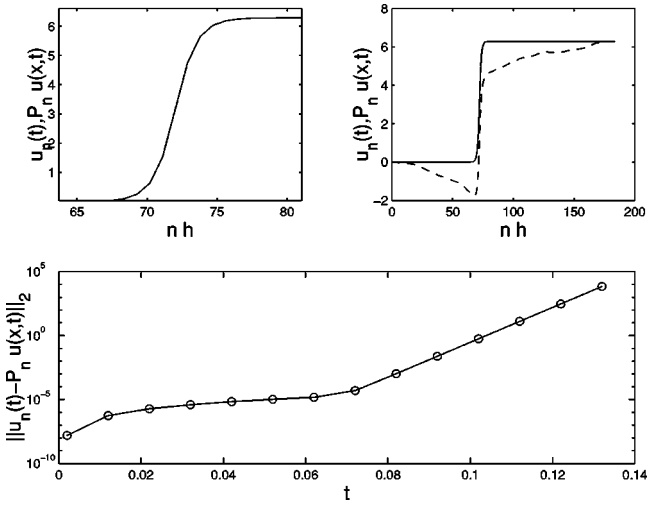

FIG. 3. The case of $h=0.9$, evaluated with the variant model with the fourth spatial derivative (which bears the potential for the "ultraviolet catastrophe"). The top left subplot shows the continuum (dashed line) and the discrete (solid line) field at $t=0.03$, while the top right subplot is at $t=0.12$. One can observe clearly in the bottom subplot of the norm difference the exponential development of the instability present in the system, which leads to completely different behaviors between the discrete and the continuum models.

tioned in Sec. III. Figure 3 shows the results for this case. The top left panel is for $t=0.03$ and the solid line of the discrete simulation is coincident with the dashed line of the continuum simulation. However, for $t=0.12$, the instability has been generated and its evolution is clearly exponential, as expected by Eq. (15), and can be observed in the semilog bottom subplot of Fig. 3 showing the norm difference between the discrete and (projected) continuum field.

In Fig. 4, the same indicators are shown as in Fig. 1, but for $h=1.3$. In this case, the discrete kink becomes trapped while the continuum ones, as can be clearly observed in the top right subplot of the kink position, continue to propagate with an approximately constant speed. The lattice spacing for which the trapping occurs is the same as the one obtained by [8], however, the important observation is that this critical value of h for the continuum models is *not* the same as in the discrete case. This is understandable in view of the absence of the PN barrier mechanism, which as we saw above is chiefly responsible, when it becomes important (i.e., for $h>1$), for the disparity between the continuum and the discrete behavior.

As was explained above, the continuum models do not accurately capture the lattice spacing at which trapping occurs. However, a natural question is whether continuum models possess the trapping property in their own right, or whether it is a genuine property of discreteness. On the one hand, bifurcations of traveling waves to standing waves have been observed in continuum systems [63], while, on the other hand, the leading-order power law [of $O(h^2)$] correction to the speed of continuum systems when they become discrete [64] is expected to be captured by the continuum

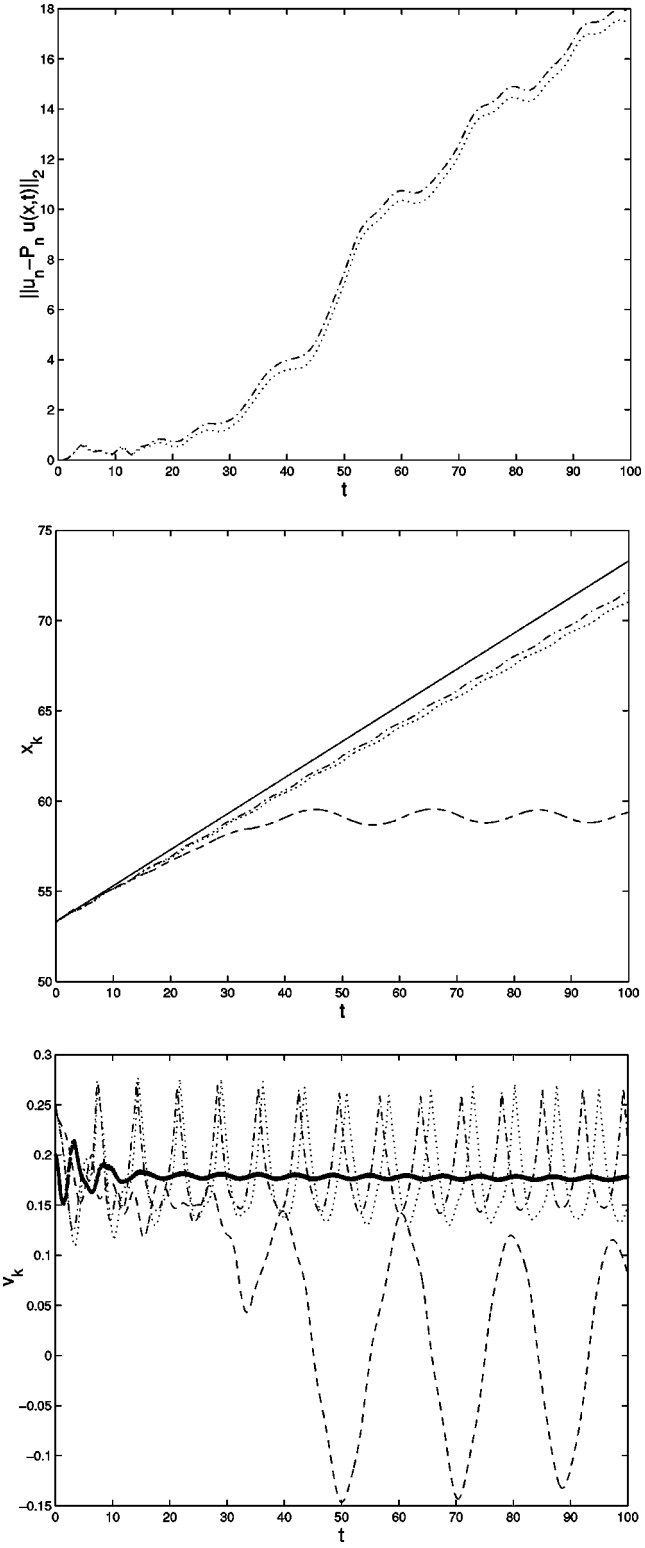

FIG. 4. Same as in Fig. 1 but for $h=1.3$. Notice that in this case the discrete kink will eventually be trapped while the continuum ones will continue propagating at an (approximately) constant average speed.

approximation, as are other such (power law) effects [23]. Furthermore, even if the PN barrier is absent, there is the shape mode oscillation, which can also resonate with the continuous spectrum and transfer some of the internal energy

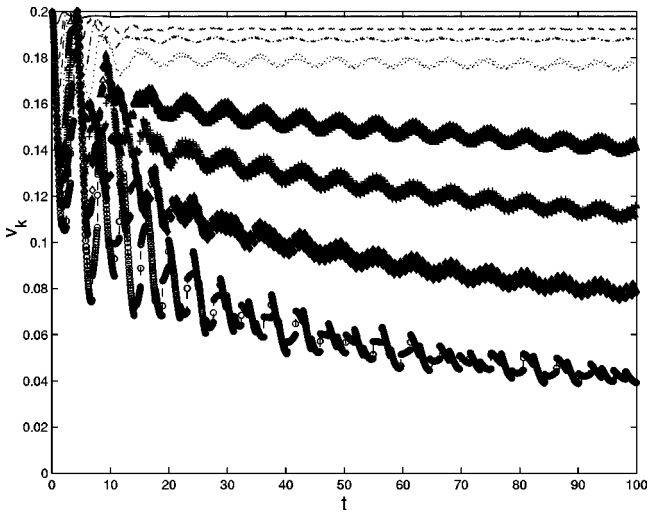

FIG. 5. This plot shows the continuum speeds of the continuum (generalized) model's kink as a function of time for different values of h. The solid line corresponds to $h=0.5$, the dashed to $h=0.9$, the dash dotted to $h=1.1$, the dotted to $h=1.3$, the triangles to $h=1.5$, the plus symbols to $h=1.6$, the diamonds to $h=1.7$, while the (lowermost) branch of circles corresponds to $h=1.8$. For $h=1.9$, propagation of the continuum kink will fail.

of the kink to phonons, thus facilitating (especially for $h>1$) the trapping process. The numerical observations of the ''continuum'' speed (defined above) confirm the contribution of all the above factors in providing a mechanism for stopping in the continuum models. The continuum speed is reduced (for low h) by a factor proportional to h^2 (in the numerical experiment the exponent is ≈ 2.1) with respect to the initial continuum speed, in agreement with [64]. As h is increased (beyond 1), higher-order effects become significant and the reduction rate of the average speed is increased, while the shape oscillation frequency also contributes more significantly to the radiation effects, as the adjustment needed for the shape of the kink is larger and hence the shape oscillation amplitude (and, hence, energy) is initially larger. In the latter case, through the coupling of the edge mode frequency harmonics to the phonon oscillations, a larger fraction of the kink's initial energy can become irreversibly delocalized [26].

As Fig. 5 demonstrates, the result of these mechanisms is the decrease of the kink speed and its eventual stopping at $h\approx 1.9$ in the case of the generalized continuum model approach, while the same phenomenon occurs for $h\approx 2.2$ in the case of the Rosenau approach.

It is interesting to note here that even though the continuum models with the Padé approximants are meant as dynamical evolution equations that share some of the features of the genuine discrete ones, one can also use them to study steady state solutions and examine the validity of semicontinuum approximations to such (static) solutions for the discrete problem. We give here a particular example of this sort. In particular, for weakly discrete models, a method was developed in [65] for finding explicit static continuum approximations to the solution of the discrete problem. In the case of the sine-Gordon equation such predictions are encompassed in Eqs. (4.4)–(4.6) of [65]. It will, thus, be true according to these predictions that the approximate static kink solution of the discrete sine-Gordon equation reads

$$u_n = w(nh) - \frac{\sin[w(nh)]}{12\beta}, \tag{29}$$

$$w(x) = -2\arctan[b\,\sinh^{-1}(bx)], x \leqslant 0, \tag{30}$$

$$w(x) = 2\pi - w(-x), x \geqslant 0, \tag{31}$$

where $b=\sqrt{1-h^2/12}$. We compare this solution to the static solution of the continuum limit

$$u_{cont} = 4\,\arctan[\exp(x)]. \tag{32}$$

We also compare the latter with the exact discrete static solution and with the continuum static kink solution of Eq. (1) when the discrete Laplacian is approximated by the Padé approximation of Eq. (17). The comparison is shown in Fig. 6 for $h=0.5$. The solid line shows the difference between the exact discrete solution and the continuum solution for h

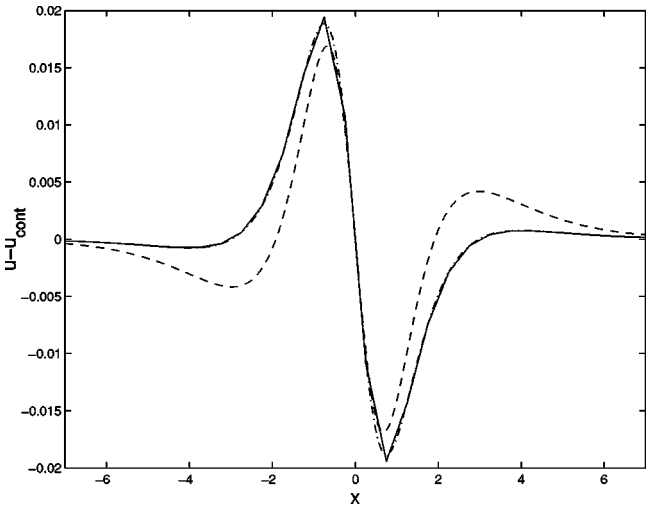

FIG. 6. This plot shows the difference between the continuum prediction for the static kink in the sine-Gordon model u_{cont} of Eq. (32) and three predictions taking discreteness into account for $h=0.5$. In particular, the solid line shows the difference between the exact discrete solution and u_{cont}; the dash-dotted line (in very good agreement with the first one) is showing the difference between the Padé approximation to discreteness of Eq. (17) and u_{cont}. Finally, the dashed line shows the difference between the weakly discrete analytical prediction of [65] and u_{cont}. The latter is also in good qualitative (but less good quantitative) agreement with the exact discrete model. The spatial profiles of these differences are shown in the figure. For a quantitative measure of the agreement see also text.

$=0.5$. The norm squared of the difference between the two is $||u_d - u_{cont}||_2^2 = 7.648 \times 10^{-4}$. The dash-dotted line is the result of the Padé approximation and can be observed to be almost exactly the same as the genuinely discrete result. In fact the $||u_{Pade'} - u_{cont}||_2^2 = 7.287 \times 10^{-4}$, also very close to the exact discrete result. Moreover, the functional dependence of these differences is almost identical. If the approximate analytical solution of [65] is compared to u_{cont}, it can be seen to capture the correct functional variation and reasonably well the quantitative details [even though the correct to $O(h^6)$ Padé approximation is more accurate]. In this case $||u_{wd} - u_{cont}||_2^2 = 5.410 \times 10^{-4}$ (the subscript stands for weakly discrete).

V. CONCLUSIONS AND FUTURE CHALLENGES

From the above results we conclude our observations in the following points.

(i) Continuum models can retain significant aspects of the phenomenology of their discrete origins. Such aspects include the dispersion relation (in the first Brillouin zone), the presence of internal modes, the same number of boundary conditions, the radiative resonances, and the slowing down and eventual pinning of the solutions.

(ii) On account of incorporating the above phenomena, these continua are expected generically to capture the properties of discrete models for h up to $O(1)$; more generally for h up to the point where the PN barrier effects will become appreciable. The PN barrier is perhaps the most significant property that continua do not share, and its exponential nature, which is significantly contributing to the pinning of discrete coherent structures, leads us to expect that the discrete and continuum equations will *not* generically have their solutions trapped at the same h. However, as we have emphasized, other features are also lost. The lack of periodicity in the dispersion relation, for instance, does not allow study of features, such as Bloch oscillations, for which such a periodicity is crucial.

(iii) The generalized approach presented herein provides a more accurate representation of the discrete case, and without considerable additional effort, higher-order schemes, which are accurate to higher power law orders, can be developed through the systematic process presented. However, as these are all power law types of (translationally invariant) corrections, the beyond all orders [25] exponential nature of the PN barrier cannot be captured. A systematic continuum way to include such exponential effects would clearly be desirable, even though it would probably have to contain an explicit spatial dependence in the continuum equation (which would break the translational symmetry).

We believe that in view of the above results, an increased understanding of the continuum approaches to discreteness has resulted and the range of validity of continuum approximations, their benefits as well as their shortcomings, have been in large part clarified. The pursuit of alternative continuum models (more amenable to mathematical analysis) that could potentially capture more closely the phenomenology of discreteness still remains a challenging task.

ACKNOWLEDGMENTS

This research was supported by the U.S. Department of Energy, under Contract No. W-7405-ENG-36, and by the National Science Foundation. Useful discussions with Yu. Gaididei, Yu. S. Kivshar, K. Rasmussen, and A. Smerzi are gratefully acknowledged. We are also particularly grateful to P. Rosenau for stimulating discussions as well as for bringing Refs. [46] and [51] to our attention.

[1] S.P. Dawson, J. Keizer, and J.E. Pearson, Proc. Natl. Acad. Sci. U.S.A. **96**, 6060 (1999).
[2] J.P. Keener, J. Theor. Biol. **148**, 49 (1991).
[3] J.P. Laplante and T. Erneux, J. Phys. Chem. **96**, 4931 (1992).
[4] A.V. Ustinov, T. Doderer, I.V. Vernik, N.F. Pedersen, R.P Huebener, and V.A. Oboznov, Physica D **68**, 41 (1993).
[5] D.N. Christodoulides and R.I. Joseph, Opt. Lett. **13**, 794 (1988).
[6] B.L. Swanson *et al.* Phys. Rev. Lett. **82**, 3288 (1999).
[7] M. Peyrard and A.R. Bishop, Phys. Rev. Lett. **62**, 2755 (1989).
[8] M. Peyrard and M.D. Kruskal, Physica D **14**, 88 (1984).
[9] Y. Ishimori and T. Munakata, J. Phys. Soc. Jpn. **51**, 3367 (1982).
[10] J.A. Combs and S. Yip, Phys. Rev. B **28**, 6873 (1983).
[11] J.P. Keener, SIAM (Soc. Ind. Appl. Math.) J. Appl. Math. **47**, 556 (1987).
[12] O.M. Braun and Yu.S. Kivshar, Phys. Rep. **306**, 1 (1998).
[13] D. Hennig and G.P. Tsironis, Phys. Rep. **307**, 334 (1999).
[14] Physica D 119, (1999), special volume edited by S. Flach and R. S. MacKay.
[15] S. Flach and C.R. Willis, Phys. Rep. **295**, 181 (1998).
[16] P.G. Kevrekidis, K.Ø. Rasmussen, and A.R. Bishop, Int. J. Mod. Phys. B **15**, 2833 (2001).
[17] R.S. MacKay and S. Aubry, Nonlinearity **7**, 1623 (1994).
[18] S. Aubry, Physica D **103**, 201 (1997).
[19] N.J. Balmforth, R.V. Craster, and P.G. Kevrekidis, Physica D **135**, 212 (2000).
[20] P.G. Kevrekidis and C.K.R.T. Jones, Phys. Rev. E **61**, 3114 (2000).
[21] T. Kapitula, P.G. Kevrekidis, and C.K.R.T. Jones, Phys. Rev. E **63**, 036602 (2001).
[22] T. Kapitula and P.G. Kevrekidis, Nonlinearity **14**, 533 (2001).
[23] Yu.S. Kivshar, D.E. Pelinovsky, T. Cretegny, and M. Peyrard, Phys. Rev. Lett. **80**, 5032 (1998).
[24] P. G. Kevrekidis, I. G. Kevrekidis, and B. A. Malomed, J. Phys. A **35**, 267 (2002).
[25] P.G. Kevrekidis, C.K.R.T. Jones, and T. Kapitula, Phys. Lett. A **269**, 120 (2000).
[26] P.G. Kevrekidis and M.I. Weinstein, Physica D **142**, 113 (2000).
[27] P. G. Kevrekidis and M. I. Weinstein (unpublished).
[28] J.P. Keener, Physica D **136**, 1 (2000).

[29] M. Johansson and S. Aubry, Phys. Rev. E **61**, 5864 (2000).
[30] P.G. Kevrekidis, I.G. Kevrekidis, and A.R. Bishop, Phys. Lett. A **279**, 361 (2001).
[31] P.G. Kevrekidis, K.Ø. Rasmussen, and A.R. Bishop, Phys. Rev. E **61**, 2006 (2000).
[32] P.G. Kevrekidis, K.Ø. Rasmussen, and A.R. Bishop, Math. Comput. Simul. **55**, 449 (2001).
[33] P.G. Kevrekidis, K.Ø. Rasmussen, and A.R. Bishop, Phys. Rev. E **61**, 4652 (2000).
[34] R. Boesch and C.R. Willis, Phys. Rev. B **39**, 361 (1989); **42**, 371 (1990); R. Boesch, P. Stancioff, and C.R. Willis, *ibid.* **38**, 6713 (1988); R. Boesch, C.R. Willis, and M. El-Batanouny, *ibid.* **40**, 2284 (1989).
[35] A. Bensoussan, J.L. Lions and G. Papanicolaou, *Asymptotic Analysis for Periodic Structures*, Studies in Applied Mathematics, Vol. 5 (Elsevier Science, Amsterdam, 1978).
[36] P.G. Kevrekidis and I.G. Kevrekidis, Phys. Rev. E **64**, 056624 (2001).
[37] P. Rosenau, Phys. Lett. A **118**, 222 (1986).
[38] P. Rosenau, Phys. Rev. B **36**, 5868 (1987).
[39] O.M. Braun, Phys. Rev. E **62**, 7315 (2000).
[40] *Padé Approximants Method and Its Applications to Mechanics*, edited by H. Cabannes (Springer-Verlag, Berlin, 1976).
[41] C. Elphick, E. Meron, and E.A. Spiegel, SIAM (Soc. Ind. Appl. Math.) J. Appl. Math. **50**, 490 (1990).
[42] Ya. Frenkel and T. Kontorova, Phys. Z. Sowjetunion **13**, 137 (1939).
[43] E.N. Pelinovsky and S.K. Shavratsky, Physica D **3**, 410 (1981).
[44] P.L. Christiansen, Y.G. Gaididei, F.G. Mertens, and S.F. Mingaleev, Eur. Phys. J. B **19**, 545 (2001).
[45] E. Hairer,S. P. Nørsett, and G. Wanner, *Solving Ordinary Differential Equations I: Nonstiff Problems* (Springer-Verlag, Berlin, 1993).
[46] See, i.e., Eqs. (15a)–(15c) of P. Rosenau, Phys. Rev. A **40**, 7193 (1989); Eqs. (3c) and (3d) *ibid.* **46**, R7371 (1992); as well as the work of C.R. Doering, P.S. Hagan, and P. Rosenau, *ibid.* **36**, 985 (1987).
[47] M.D. Kruskal and N.J. Zabusky, J. Math. Phys. **5**, 231 (1964).
[48] S. Pnevmatikos, N. Flytzanis, and M. Remoissenet, Phys. Rev. B **33**, 2308 (1986).
[49] N. Flytzanis, St. Pnevmatikos, and M. Remoissenet, J. Phys. C **18**, 4603 (1985).
[50] A. Champneys and Yu.S. Kivshar, Phys. Rev. E **61**, 2551 (2000).
[51] Recently, it was brought to our attention by P. Rosenau that he considered expressions of the form of Eq. (19) in Prog. Theor. Phys. **79**, 1028 (1988). The latter considerations were not motivated by continued fraction generalizations but rather by the necessity to treat anomalous effects in the dispersion relation arising, for example, in the case where next nearest neighbor interactions are present. In this case, the regularization led to equations with sixth-order mixed derivatives (fourth order in space and second order in time).
[52] D. Cai, A.R. Bishop, and N. Gronbech-Jensen, Phys. Rev. Lett. **72**, 591 (1994).
[53] J. Hirth and J. Lothe, *Theory of Dislocations* (Wiley, New York, 1982).
[54] V. I. Arnold, *Mathematical Aspects of Classical Mechanics* (Springer-Verlag, New York, 1989).
[55] D. Cai, A.R. Bishop, and N. Gronbech-Jensen, Phys. Rev. E **53**, 4131 (1996).
[56] T. Kapitula, P.G. Kevrekidis, and B.A. Malomed, Phys. Rev. E **63**, 036604 (2001).
[57] A. Trombettoni and A. Smerzi, Phys. Rev. Lett. **86**, 2353 (2001).
[58] R. Scharf and A.R. Bishop, Phys. Rev. A **43**, 6535 (1991).
[59] D. Cai, A.R. Bishop, N. Gronbech-Jensen, and M. Salerno, Phys. Rev. Lett. **74**, 1186 (1995).
[60] J. Feldmann *et al.*, Phys. Rev. B **46**, 7252 (1992).
[61] M. Holthaus, Phys. Rev. Lett. **69**, 351 (1992).
[62] B.P. Anderson and M.A. Kasevich, Science **282**, 1686 (1998).
[63] I.G. Kevrekidis, B. Nicolaenko, and J.C. Scovel, SIAM (Soc. Ind. Appl. Math.) J. Appl. Math. **50**, 760 (1990).
[64] S. Heinze, G. Papanicolaou, and A. Stevens, SIAM J. Appl. Math. **62**, 129 (2001).
[65] S. Flach and K. Kladko, Phys. Rev. E **54**, 2912 (1996).